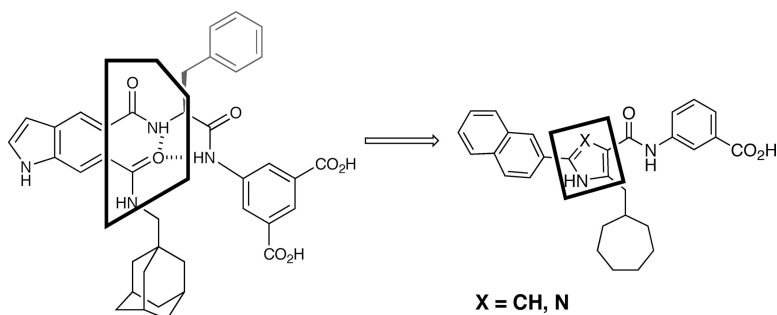


Scaffold Hopping with Molecular Field Points: Identification of a Cholecystikin-2 (CCK) Receptor Pharmacophore and Its Use in the Design of a Prototypical Series of Pyrrole- and Imidazole-Based CCK Antagonists

Caroline M. R. Low, Ildiko M. Buck, Tracey Cooke, Julia R. Cushnir, S. Barret Kalindjian, Atul Kotecha, Michael J. Pether, Nigel P. Shankley, J. G. Vinter, and Laurence Wright

J. Med. Chem., **2005**, 48 (22), 6790-6802 • DOI: 10.1021/jm049069y • Publication Date (Web): 11 October 2005

Downloaded from <http://pubs.acs.org> on March 29, 2009



More About This Article

Additional resources and features associated with this article are available within the HTML version:

- Supporting Information
- Links to the 8 articles that cite this article, as of the time of this article download
- Access to high resolution figures
- Links to articles and content related to this article
- Copyright permission to reproduce figures and/or text from this article

[View the Full Text HTML](#)

Articles

Scaffold Hopping with Molecular Field Points: Identification of a Cholecystokinin-2 (CCK₂) Receptor Pharmacophore and Its Use in the Design of a Prototypical Series of Pyrrole- and Imidazole-Based CCK₂ Antagonists

Caroline M. R. Low,^{*,†} Ildiko M. Buck,[†] Tracey Cooke,[†] Julia R. Cushnir,[†] S. Barret Kalindjian,[†] Atul Kotecha,[†] Michael J. Pether,[†] Nigel P. Shankley,^{†,‡} J. G. Vinter,[§] and Laurence Wright[†]

James Black Foundation, 68 Half Moon Lane, London, SE24 9JE, U.K., and Cresset BioMolecular Discovery Ltd., Spirella Building, Bridge Road, Letchworth, Herts, SG6 4ET, U.K.

Received November 18, 2004

A new molecular modeling approach has been used to derive a pharmacophore of the potent and selective cholecystokinin-2 (CCK₂) receptor antagonist **5** (JB93182), based on features shared with two related series. The technique uses “field points” as simple and effective descriptions of the electrostatic and van der Waals maxima and minima surrounding a molecule equipped with XED (extended electron distribution) charges. Problems associated with the high levels of biliary elimination of **5** in vivo required us to design a compound with significantly lower molecular weight without sacrificing its nanomolar levels of in vitro activity. Two new series of compounds were designed to mimic the arrangement of field points present in the pharmacophore rather than its structural elements. In a formal sense, two of the three amides in **5** were replaced with either a simple pyrrole or imidazole, while some features thought to be essential for the high levels of in vitro activity of the parent compounds were retained and others deleted. These compounds maintained activity and selectivity for this receptor over CCK₁. In addition, the reduction in molecular weight coupled with lower polarities greatly reduced levels of biliary elimination associated with **5**. This makes them good lead compounds for development of drug candidates whose structures are not obviously related to those of the parents and represents the first example of scaffold hopping using molecular field points.

Introduction

We have reported several novel classes of cholecystokinin-2 (CCK₂) receptor antagonists that all show good selectivity for this receptor over the closely related CCK₁ receptor.¹ These have included compounds based on substituted dibenzobicyclo[2.2.2]octanes (BCO),² two related series based on bicyclic aromatic scaffolds,^{3,4} and a series of novel benzo[*h*][1,4]diazonines.⁵ The two subclasses of cholecystokinin receptors mediate a wide range of peripheral and central biological processes, and identification of selective ligands for either subtype has attracted a large amount of interest.^{6–10} CCK₁ receptors occur centrally in the *nucleus tractus solitarius*¹¹ but are mainly located in the pancreas,¹² gall bladder,¹³ and colon. CCK₂ receptors are the predominant subtype in the brain and are widely distributed throughout the cortex.¹⁴ They are also located on the ECL cell of the stomach where they are involved in the regulation of gastric acid secretion. There is strong evidence to suggest that the central and peripheral populations of receptors are homogeneous, on the basis of their selectivity for a range of ligands and evidence from molecular

hybridization studies.¹⁵ Both human CCK₁ and CCK₂ receptors have been cloned and shown to belong to the family of G-protein-coupled receptors.^{15–18} The problems associated with designing drug candidates for the major class of G-protein-coupled receptors (GPCRs) that are activated by peptides are well described. In such cases it is imperative that compounds should not be peptidic because of the recognized problems of potential immunogenicity, low metabolic stability, and bioavailability associated with this class of molecule. However, the search for suitable small-molecule candidates is also hampered by the lack of detailed knowledge about the structure of the receptors themselves. Hence, we are limited to indirect methods of determining the requirements of high-affinity ligands for our target receptor protein, in this case the CCK₂ GPCR.

Conventional molecular modeling techniques place a high emphasis on using structural comparisons as their basis for explaining patterns of biological activity. These methods have had some success in rationalizing the behavior of closely related compounds but place significant constraints on the development of distinct new molecular entities. For example, the hormone CCK is a large peptide and compounds described as competitive CCK₂ antagonists represent a diverse group of small-molecule non-peptides ranging from benzodiazepines, such as L-365,260¹⁹ and YF476,²⁰ to peptoids, such as

* To whom correspondence should be addressed. Phone: +44 20 7737 8282. Fax: +44 20 7274 9687. E-mail: caroline.low@kcl.ac.uk.

[†] James Black Foundation.

[‡] Current Address: Johnson & Johnson Pharmaceutical Research & Development, LLC, 3210 Merryfield Row, San Diego, CA 9212.

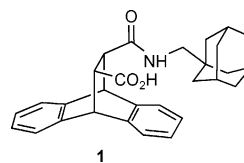
[§] Cresset BioMolecular Discovery Ltd.

PD134308,²¹ to our own bicyclic aromatics, typified by **5**.⁴ All of these compounds are selectively recognized by the CCK₂ receptor, and if we assume, in the absence of any experimental evidence to the contrary, that they bind to a similar site on the receptor, then we should be able to identify common features relating one to another. Analyzing their structures alone does not provide us with a unifying rationale that would allow us to move directly from one series to another. However, the receptor binds all of these structures with nanomolar affinity, suggesting that it uses additional features to recognize and interact with ligands. This observation is not confined to CCK₂ receptor ligands and we are not alone in believing that the processes of molecular recognition and binding are governed by electrostatic and steric features that are not explicitly represented in the stick representations of molecular models. It therefore follows that if two molecules with diverse structures can generate similar electronic properties in a particular conformation, they will interact with an enzyme or receptor in a similar way. This point is recognized in other modeling techniques to some extent, e.g., GRID analysis²² and other methods of pharmacophore modeling.^{23,24} However, it is difficult to apply these to automated analysis of diverse structures because many require significant operator input to generate alignments.

This conundrum has led us to develop a new molecular modeling approach that uses "field points" as simple and effective descriptions of the electrostatic and van der Waals maxima and minima surrounding a molecule.²⁵ Sets of field points are calculated for individual conformations equipped with XED (extended electron distribution) charges²⁶ rather than the atom-centered charge descriptions used in conventional molecular mechanics packages. The XED concept was originally based on results obtained by Hunter and Sanders who showed that a three-center charge model could be used to reproduce the stacking geometry of porphyrins better than an equivalent atom-centered charge model.²⁷ We have now extended this approach and derived a new molecular mechanics force field in which appropriately parametrized XED charges have been added to the Coulombic term. The package has been evaluated against experimental data compiled by Guntertofte et al.^{28,29} and found to be superior to most of the commercially available packages.³⁰ This was particularly true in the case of aromatic–aromatic π -stacking interactions and examples where the anomeric effect controls the choice of conformational space.

The field points that we have developed are based on the widely used molecular electrostatic potential (MEP) descriptors but resemble the results of distributed multipole analysis when derived using XED charges. However, accurate calculation of MEPs requires the use of quantum mechanical methods, making their derivation time-consuming. We have found that the quality of molecular electrostatic maps obtained using simpler molecular mechanics methods can be improved using XED charge descriptions. Further simplification has been achieved by distilling these maps down to their energy extrema, which we have termed field points. A new method of defining surface interaction has been added, and the resulting composite maps can be rapidly

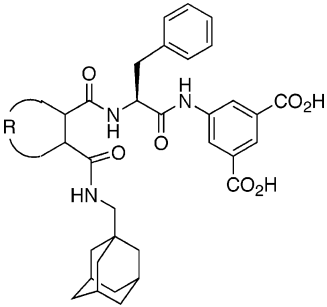
Chart 1. CCK₂ Antagonist Based on the Dibenzobicyclo[2.2.2]octane (BCO) Core

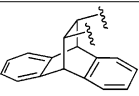
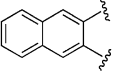
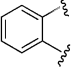
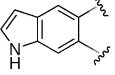


derived for sets of low-energy conformations of the compound of interest. Sets of field points can be easily compared with one another and the resulting overlay displayed together with its structural origin, facilitating interpretation of the results in chemical terms. This approach avoids the problems of choosing structural alignments that limit conventional QSAR methods, such as CoMFA.^{24,31} In addition, the comparison of individual sets of field points is a fast process, making it feasible to compare many conformations of the same molecule against those of another. Conversely, methods for comparing molecular similarity using MEPs are generally more involved and many require significant manual manipulation in generating the final overlay.³² The first examples using this field point approach were reported some time ago,²⁵ and this paper will describe its application to the design of a new series of CCK₂ receptor antagonists.

Our first examples of CCK₂ antagonists, typified by structure **1** (Chart 1), all contained a BCO core and had micromolar affinity for this receptor.² They were the products of functionalizing the two bridgehead positions with an alicyclic amide and a carboxylate, respectively. A series of structural modifications rapidly showed that both the activity and selectivity of these compounds could be improved by extending the carboxylate side-arm. This gave compounds, such as **2**, with the same levels of CCK₁ affinity but whose affinity for CCK₂ receptors had increased by a factor of 100 (Table 1). The optimal substituents were found to be 1-adamantylmethyl on one arm, with the 3,5-dicarboxyanilide derivative of L-Phe on the second.³ The bulky BCO was not a unique requirement and could be replaced by simple aromatic groups to give compounds with 10- to 30-fold lower activity (**3** and **4**). However, field point analysis of the original BCO series had suggested that a key feature of these compounds was not present in the naphthalene analogue **3**. Both molecules had a series of electropositive field points of varying magnitude around the plane of the aromatic groups. In addition, the BCO **2** also had a sizable negative field point arising from the focus of the π -electrons of the two isolated aromatic rings. This led us to devise the indole derivative **5**, which we compared to BCO **2** using our field point overlay methodology, as previously described.⁴ The desired relationship was maintained in most of the pairwise comparisons generated. Compound **5** was synthesized and our expectations were confirmed when it was shown to possess a profile of activity that was indistinguishable from that of the BCO **2** in a number of *in vitro* bioassays. This was clearly a significant finding and demonstrated that this methodology could be used in a meaningful fashion.

At this point we had access to a family of three compounds (**2**, **3**, and **5**) that differed in the nature of the group to which the two amide sidearms were

Table 1. Biological Data for Compounds Incorporated in the CCK₂ Receptor Pharmacophore


No	R	CCK ₂ ^a pKi ± s.e.m	CCK ₁ ^a pKi ± s.e.m.
2		8.8 ± 0.1 ^b	5.7 ± 0.1 ^b
3		7.9 ± 0.1 ^c	6.1 ± 0.1 ^c
4		7.5 ± 0.3	5.5 ± 0.1
5		9.0 ± 0.2 ^c	5.4 ± 0.2 ^c

^a Compounds were tested as the bis(*N*-methyl-D-glucamine) salts. ^b Reference 3. ^c Reference 4.

anchored. However, we were also aware that representative examples of these compounds were rapidly excreted, unchanged, in the bile of both rats and dogs. This presented us with the challenge of designing new molecules with improved bioavailability while retaining the high levels of potency and selectivity for CCK₂ receptors that had been demonstrated in vitro. Biliary excretion is a complex process whose mechanism is still not fully understood. However, a possible cause for this rapid clearance was the high molecular weights of these compounds that, at around 700, were significantly above the qualitative threshold of 325 that is commonly quoted for biliary excretion in these two species. This threshold is known to be species-dependent and rises to a value of between 500 and 600 in man. However, it is well recognized that removing molecular weight from ligands without concomitant loss of activity is not a simple task.³³

A number of “scaffold-hopping” approaches have been described in the literature. This recent concept involves the computational comparison of chemical scaffolds to generate new chemical entities with different molecular frameworks. The overall aim is to change the physical characteristics of a drug candidate to avoid adverse properties or create compounds whose structural relationship to the starting point is not obvious. A number of examples of cannabinoid receptor antagonists, whose structures cannot be categorized as bioisosteres or conformationally constrained analogues of rimonabant, have been recently reviewed, although the processes underlying their discovery are not discussed in any detail.³⁴ Software for the de novo design of new estrogen

receptor ligands, in the absence of information about the receptor, has been described;³⁵ however, no biological data were presented for any of the structures proposed. An alternative approach used “fuzzy” molecular representations called FEPOPS (3D feature point pharmacophores) to suggest new leads based on compounds already present in an in-house high-throughput-screening database.³⁶ All of these approaches require the definition of a pharmacophore, and hence, our first step was to define such a model for compounds **2**, **3**, and **5**, based on our existing knowledge, which might be used to indicate ways in which the rapid biliary excretion observed in vivo could be reduced without compromising the high levels of in vitro activity that had already been achieved.

Chemistry

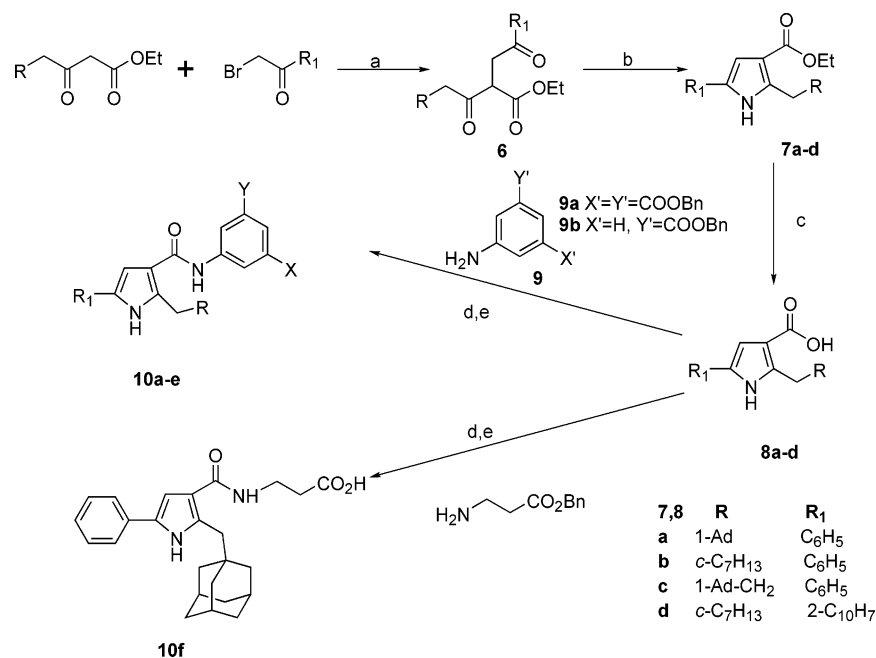
The pyrrole derivatives in Table 3, **10a–f**, were prepared according to the general route in Scheme 1. Pyrroles **7a–d** were prepared from the diketoesters (**6**) following literature procedures.^{37,38} Hydrolysis of the ethyl ester of intermediates **7a–d** afforded the acids **8a–d**, which were coupled with aminoisophthalic acid dibenzyl ester (**9a**) or 3-aminobenzoic acid benzyl ester (**9b**) via their acid chlorides to afford **10a–e**, after hydrogenolysis of the benzyl ester protecting group. Reaction of the acid chloride formed from **8a** with β -alanine benzyl ester afforded **10f** after hydrogenolysis.

The imidazole derivatives **17a–g** were prepared by the general route outlined in Scheme 2. Tricarbonyls **13** were prepared by oxidation³⁹ of ylides **12**⁴⁰ and converted to the trisubstituted imidazole carboxylic acids **15a–e** by reaction with benzaldehyde or 2-naphthaldehyde in the presence of acetic acid/ammonium acetate,⁴¹ followed by hydrolysis of the ethyl ester. Coupling of the aniline derivatives **9a–c** to the acids **15a–e** under standard active ester coupling conditions, followed by the appropriate deprotection, afforded **17a–g**. All the compounds were tested as *N*-methyl-D-glucamine salts. The salts were prepared by stirring a mixture of the compound with 1 or 2 equiv of *N*-methyl-D-glucamine, as appropriate, in dioxan–water (1:1) until a solution was obtained. The solution was then freeze-dried, and all compounds were obtained as fluffy white solids.

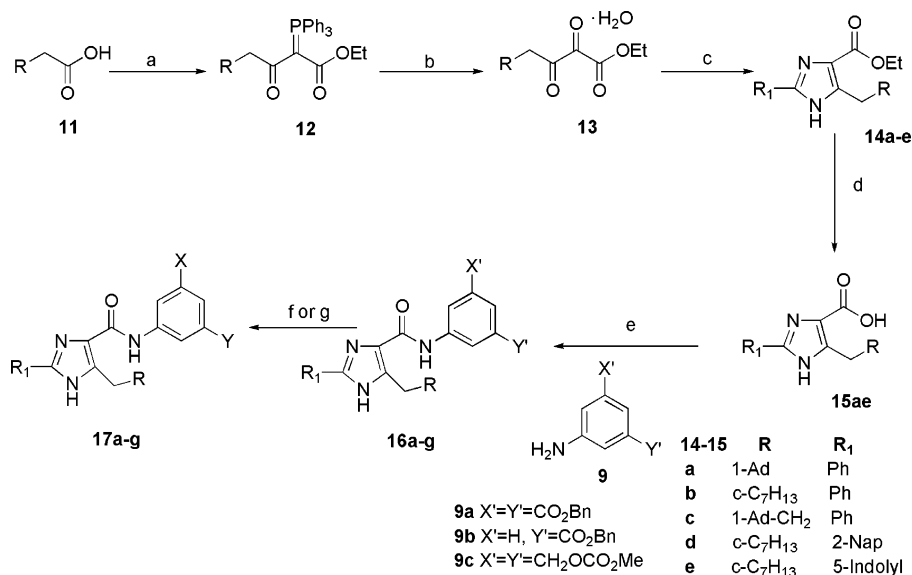
Molecular Modeling

Molecular modeling analyses were carried out using structures equipped with XED charges rather than conventional atom-centered charges. We have found that this modification allows us to reproduce experimental thermodynamic data with good accuracy³⁰ and have incorporated these charge descriptions into our standard modeling package, XED.⁴²

In this study, structures were selected on the basis of their biological activity with the emphasis on antagonists with nanomolar affinity and good selectivity for CCK₂ over the closely related CCK₁ receptor (Table 1). Each compound was submitted to a conformational hunting routine in order to generate a set of conformations equipped with XED charges and field points whose energies lay within 3 kcal/mol of the calculated global minimum. This limit was chosen, in line with accepted practice,⁴³ because the Boltzmann equation predicts that

Scheme 1. Synthesis of Trisubstituted Pyrroles^a

^a (a) K₂CO₃, NaI, Me₂CO; (b) NH₄OAc, AcOH; (c) NaOH, EtOH-H₂O; (d) SOCl₂, pyr; (e) Pd-C, H₂, THF-MeOH.

Scheme 2. Synthesis of Trisubstituted Imidazoles^a

^a (a) Ph₃PCH=CO₂Et, EDC, DCM; (b) OXONE, THF-H₂O; (c) R₁CHO, NH₄OAc, AcOH; (d) NaOH, EtOH-H₂O; (e) EDC, HOBT, DMF; (f) Pd-C, H₂, THF-MeOH when X' = Y' = CO₂Bn or X' = H and Y' = CO₂Bn; (g) 1% K₂CO₃, THF-MeOH when X' = Y' = CH₂OCO₂Me.

<1% of available conformations will have energies greater than 3 kcal/mol above the lowest energy conformation found at body temperature, i.e., 37 °C (310 K). This process typically gave a set of 10–40 conformations for each molecule.

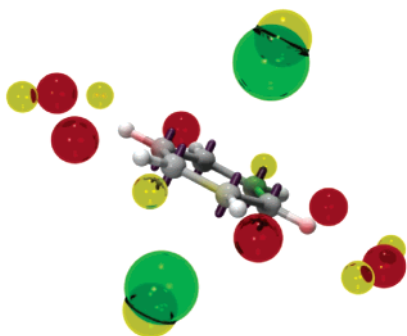
Conformational Hunting

The protocol used was as follows. Calculations were carried out at dielectric constant of 2.0, allowing all rotatable bonds to move. An initial set of conformations was generated using a hard spin torsional minimizer. Each input conformation was randomized 250 times (Monte Carlo), twisting each bond by 10° torsional increments, iterating through all bonds to 0.001 cal/mol and storing all conformations within a 15.0 kcal/mol range of the lowest energy structure found. Conforma-

tions within 15° on all torsions of any other were removed. The energies of all remaining structures were then minimized using a combined parabolic/Fletcher-Reeves conjugate gradient technique, whose accuracy was set at <0.01 cal/mol. XED charges were then added to each conformation, and the energies of each structure were minimized once again using the same procedure. Conformations were collected over a 15.0 kcal/mol energy range to a maximum of 1000 structures.

Calculation of Field Points

Three classes of field point were generated for each conformer: positive and negative electrostatic extrema and a third class of “sticky” points defining the van der Waals surface around the molecule. The electrostatic field points are calculated using a constant point unit

Scheme 3. Molecular Field Points Calculated for Benzene^a

^a The aromatic carbon atoms are equipped with XED charges (purple). Positive and negative electrostatic points are shown in red and green, respectively, and van der Waals points are shown in yellow. The size of the spheres is directly related to the magnitude of the field point.

charge, the size of an oxygen atom, of +1 for a positive probe and -1 as a negative probe. The probes are placed on a grid of points 3 Å above the molecular van der Waals surface at a dielectric constant of 4.0. Full details of the methodology used have been published elsewhere.²⁵ The interval between grid points is adjusted so that the whole molecular surface is covered using a maximum of 250 points. This number varies according to the compromise between the interval and the area of the molecule.

After allocation of an interaction energy to every grid point, each point is allowed to find its appropriate maximum or minimum, using a 3D simplex algorithm that is now no longer confined to the grid itself. The result is that many minimized positions eventually coincide. After coincident extrema are filtered out, the final positions of the field points are stored, together with their type (positive or negative) and energy (well-depth) information. These are plotted around the molecule as red (positive) and green (negative) spheres whose radii reflect the depth of the energy well. The final set of unique extrema is stored with Cartesian coordinates, the field point class, and the interaction well depth in energy units.

The results can be readily understood by considering the pattern of field points generated for a molecule, such as benzene (Scheme 3). In this case negative points are found in the expected location of the π -electrons with a ring of smaller positive points in the plane of the ring. A third class of "sticky" points, shown in yellow, is calculated using a neutral probe and a Morse potential to represent the van der Waals properties of the molecule. These broadly map the surface of the molecule and suggest where the "stickiest" points occur.

An earlier description of this procedure has been published²⁵ and differs only in that all probe classes use a Morse equation for the van der Waals interactions. A simple Coulombic term is used for the electrostatic probes.

Comparison of Ligands Using Field Points

The set of field points generated for a particular conformation of a ligand (A) was compared to all the conformers of another molecule (B) on a pairwise basis. This process involved inverting the charges of the field

points on one molecule and driving them over those of the second under a Coulombic potential. The process was then reversed such that A was compared with B, and B with A. The interaction between the two molecules can then be quantified in terms of a scoring function, which we have termed the "overlay energy", that is calculated as q_1q_2/r^2 (where r is the distance between two charges q_1 and q_2). This number reflects the degree of similarity between the two sets of field points. Thus, comparisons between pairs of molecules are made entirely on the basis of the field points, avoiding the problems of operator bias in choosing structural alignments, a recognized limit of conventional QSAR methods such as CoMFA.^{24,31} Goodness-of-fit was ranked on the basis of the "overlay energy" parameter, and the 50 best overlays, i.e., those with the lowest overlay energies, were stored. A complete comparison of 20 conformations of **2** with six conformations of **5** took 1 h to reach completion on a Silicon Graphics Octane with dual 270 MHz IP30 processors.

Biology

CCK₂ receptor activity was assessed by testing all compounds in a radioligand binding assay in mouse cortical membrane homogenates, in competition with 20 pM [¹²⁵I]BH-CCK-8S, as previously described.⁴⁴ The $pK_i \pm$ SEM values were determined using results taken from at least three separate experiments. Activity at CCK₁ receptors was established using an equivalent assay in guinea pig pancreas cell homogenates.⁴⁵ In the same way $pK_i \pm$ SEM values were determined in competition with 20 pM [¹²⁵I]BH-CCK-8S, using results taken from at least three separate experiments.

The agonist/antagonist properties of two compounds, **10a** and **17c**, were examined in the isolated, lumen-perfused immature rat stomach.⁴⁶ $pK_B \pm$ SEM values were estimated from single shifts of pentagastrin *t*Boc-CCK(29-33) concentration-effect curves, calculated assuming an underlying Schild slope of unity and fitted using the Gaddum-Schild equation.

Biliary elimination was measured in anesthetized rats as the percentage of unchanged compound detected in the bile following iv bolus administration of the compound at a dose of either 1 or 10 μ mol/kg. The bile duct was cannulated and bile collected over 15 min intervals for a total 150 min in each case. The unchanged compound was detected by reverse-phase HPLC (Waters C8 column), eluting with H₂O/CH₃CN (30:70) + 0.01% CH₃COOH (final pH 3.74) and monitoring at 286 nm.

Results and Discussion

We have already demonstrated the use of our field point methodology in moving from the original BCO series to the heterocyclic derivatives typified by indole **5**.⁴ However, there is a clear structural relationship between these compounds, and significant synthetic effort had already shown that certain groups could not be removed from these optimized structures without concomitant loss of biological activity. This made it difficult to envisage ways in which we could include those features that we knew to be essential for the high levels of in vitro activity in a compound with greatly reduced molecular weight.

One of the advantages of using field points to summarize molecular properties is that it allows us to

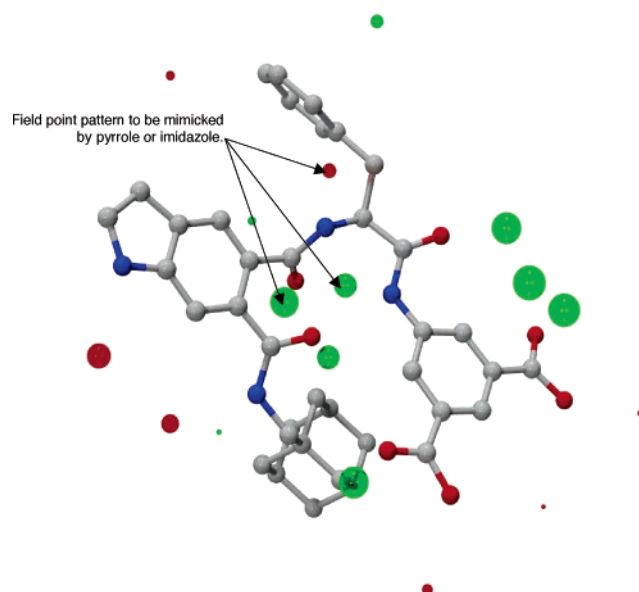
separate elements responsible for recognition and receptor binding from their structural origins. This led us to hope that we could introduce much greater levels of diversity into our design process once we removed the need to reproduce structural features directly. The first step in this process was to define a field point pharmacophore that encompassed the properties of the current series. We chose to construct this from compounds **2**, **3**, and **5**, each equipped with the optimal choice of side-arms but with different nuclei. The affinities of these compounds are not identical; however, they all behave as competitive antagonists in the presence of pentagastrin,^{2–4} and so we assume, since we have no evidence to the contrary, that they bind to the same site on the CCK₂ receptor. Our aim was to use molecular field point analysis to identify conformations of **2**, **3**, and **5** with the most similar electronic properties as a way of identifying a ligand-based pharmacophore.

To this end, 22 conformations of the naphthalene **3** were compared with 6 generated for the indole **5**. The results showed that the arrangement with the lowest “overlay energy” was an essentially unique conformation of the amidic side chains in which the adamantyl and 3,5-dicarboxyanilide groups were held in proximity by the presence of a bifurcated H-bond between the carbonyl oxygens of the geminal amides and the anilide NH. This provided the first clue to the bioactive conformation of **3** and **5**. Furthermore, we could test this proposal by comparing indole **5** to BCO **2** on the same basis. In this case the best field point overlay occurred with the same conformation of indole **5** and a conformation of BCO **2** that also fitted the previous observations. At this point we should stress that the comparison was not biased by seeding the results with the common structure identified in the first experiment but resulted from the exhaustive comparison of the complete set of conformations generated for a 3 kcal/mol range in each case.

Because this study was one of the first applications of the field point methodology, we restricted our original choice of compounds to those that were generated in house and fully characterized as competitive antagonists. The levels of structural diversity within this set are not high but are analogous to those of most data sets used in CoMFA analyses, where a significant portion of the structure must be common to allow the operator to manually superpose the molecules in the training set. We have subsequently extended this approach to include other examples of the diverse set of known CCK₂ receptor ligands, such as the peptoid PD134308⁴⁷ and the benzodiazepine YF476.²⁰ The conformation of indole **5** identified in these later studies does not differ significantly from that described here (unpublished results).

The conformation of indole **5** identified by this process shows a number of interesting features. For example, the polar 3,5-dicarboxyanilide is located close to the hydrophobic adamantyl, although we might have expected to find this group associated with one of the other hydrophobic components of the molecule (Scheme 4). This arrangement is maintained by hydrogen-bonding between the amides of the two arms and is mirrored in all the low-energy structures. The pattern of field points around the molecule illustrates that the system is

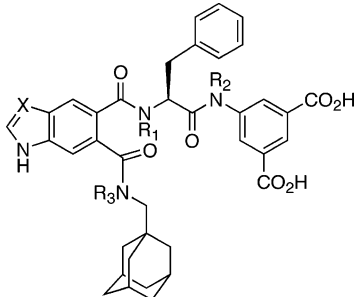
Scheme 4. Proposed Bioactive Conformation of Indole **5**^a



^a Identified by field point comparison of multiple conformations of BCO **2**, naphthalene **3**, and indole **5**. Electrostatic field points are shown in red (positive charge) and green (negative charge), but van der Waals points have been omitted for clarity. The field point pattern due to the Phe residue and the amidic carbonyl of the adjacent adamantylmethyl sidearm are highlighted.

broadly dipolar, in common with our model of the tetrapeptide fragment *t*Boc-CCK(30–33) on which the design of the original series of BCOs was based.⁴⁸ It is not surprising that the groups that contribute most to the population of negative field points are the carbonyls of the amides and carboxylic acids. However, there is also a significant density of positive field points generated by the edge of this electron-deficient indole system and the NH adjacent to the adamantyl group.

The next step was to seek physical evidence for the existence of this structure. A series of ¹H NMR experiments (in DMSO-*d*₆) was carried out on indole **5** and several closely related analogues. These showed a number of consistent features that supported our proposed structure. For example, both the nuclear Overhauser enhancement (NOE) difference and rotating-frame Overhauser enhancement spectroscopy (ROESY) experiments showed evidence of the proximity of the ortho protons of the aniline dicarboxylate to the adamantane methylenes. There were also a number of ROEs between the phenyl protons of the Phe residue and the indole group but none to the aniline, suggesting that the Phe side chain bends back toward the heterocycle. This is also supported by the existence of NOEs between the β -methylene protons of the Phe and the ortho protons of the aniline. In addition, there were strong NOEs between the amide NH adjacent to the adamantyl and the 7-CH of the indole, defining the configuration of this sidearm. These findings are all in line with our proposed structure and rule out several other possible conformations. For example, the set of conformations generated for indole **5** contains a number of structures in which the 3,5-dicarboxyanilide is folded back over the indole group. The existence of this conformation would be reflected by the presence of NOEs between the protons attached to the aniline and

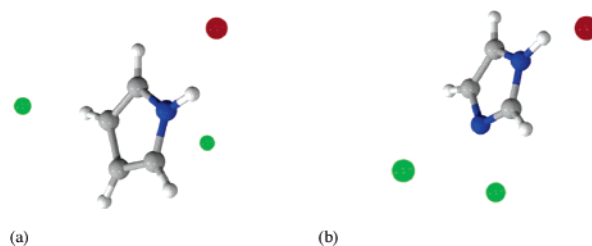
Table 2. Effect of N-Methylation of the Individual Amides on the Activities of Indole **5** and Benzimidazole **18**


compd	X	R ₁	R ₂	R ₃	loss of CCK ₂ activity relative to parent (log units)		CCK ₁ ^a pK _i ± SEM
					CCK ₂ ^a pK _i ± SEM		
5	CH	H	H	H	9.0 ± 0.2		5.4 ± 0.2
18	N	H	H	H	8.3 ± 0.1		5.8 ± 0.3
19	N	Me	H	H	7.6 ± 0.1	0.7	5.0 ± 0.2
20	N	H	Me	H	6.3 ± 0.1	2.0	5.4 ± 0.2
21	CH	H	H	Me	7.8 ± 0.1	1.2	5.7 ± 0.2

^a Compounds were tested as the bis(*N*-methyl-D-glucamine) salts.

the indole group. None of the ¹H NMR experiments carried out to date have provided any evidence of the existence of such a population in solution.

Hence, we have gathered some evidence that indole **5** can adopt the topology in solution that we propose for our pharmacophore. Additional evidence of the nature of the bioactive conformation was supplied by the results of chemical modification of the indole **5** and the closely related benzimidazole analogue **18**. The overall conformation of the proposed pharmacophore is stabilized by hydrogen bonding between the carbonyl oxygens and NHs of the various amides. In fact, two conformations of similar energy have been identified from our modeling experiments. One involves the interaction of the Phe and anilide NHs with the carbonyl group of the adamantyl amide, as shown in Scheme 4, and the second relies on hydrogen bonding between the oxygens of the two amide carbonyl groups attached to the indole and the anilide NH. The energy difference between these two alternatives is 1 kcal/mol, and so the Boltzmann equation predicts that the ratio of the two conformations will be 5:1 in favor of the first, lower energy conformation at 37 °C. The role that the various amides play in maintaining the overall structure was further probed by methylation of the individual NHs (**19–21**). Molecular modeling showed that methylation of either the anilide or adamantylmethylamide NHs reinforced the H-bond between the NH of the Phe and the carbonyl oxygen of the adamantylmethylamide. However, interpreting these results was not straightforward because methylation of either of the amide NHs on the side chain attached to the 5-position of the indole group changed the configuration of the relevant amide bond from *E* to *Z*. In practice the compounds synthesized showed a loss of CCK₂ activity in all cases (Table 2). It is also interesting to note that levels of CCK₁ affinity remained constant throughout this exercise. The most pronounced effects were noted when the anilide NH was methylated (**20**), resulting in a 100-fold loss of activity. This result does not allow us to distinguish between the

Scheme 5. Electrostatic Field Point Patterns Calculated for (a) Pyrrole and (b) Imidazole Equipped with XED Charges^a

^a Negative points are shown in green, and positive points are shown in red.

two H-bonding possibilities but supports our belief that this group is essential to maintaining the overall structure of the series. Smaller losses were observed on methylation of the Phe NH in **19** and adamantyl amide NHs in **21**.

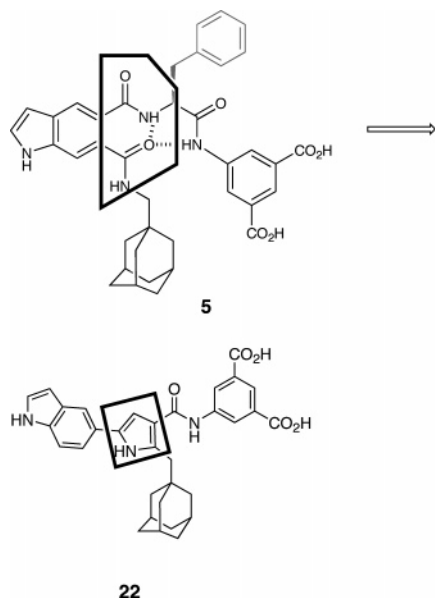
Structure–activity studies had convinced us that the most important features of indole **5** were the hydrophobic adamantyl group, the heteroaromatic group, and the 3,5-dicarboxyanilide.⁴ Furthermore, we believed that we had identified two possible bioactive conformations of this compound and had access to both structural and field point representations of this pharmacophore. We were now in a position to exploit this information in the design of novel compounds. Our strategy was to tackle the problem of biliary elimination by reducing the molecular weight of the structure without sacrificing the high levels of *in vitro* activity that had already been attained.

Molecular mechanics calculations had repeatedly shown that there was a consistent spatial relationship between the three constituents of indole **5** to which we alluded earlier. However, we had been unable to pin down a role for the Phe side chain, which showed a high degree of conformational mobility. In addition, structure–activity studies had shown that the side chain of the amino acid incorporated at this point could be altered substantially without significant effect on the affinity of the compounds.⁴ Hence, we decided to omit this group from our initial survey of potential candidates in the interests of reducing their overall molecular weight.

We also considered that it might be possible to reflect the properties of the three amides responsible for maintaining the proximity of the adamantyl and 3,5-dicarboxyanilide with a small rigid heterocycle. Careful analysis of the pattern of electrostatic field points generated by the two amide groups attached to the indole showed that there were three significant field points, one positive and two negatives (Scheme 4), to be considered. Good candidates for this purpose appeared to be either pyrrole or imidazole because the electrostatic field point patterns around each of these is consistent with the pattern attributed to the amides linking the Phe residue and its adjacent sidearm to the indole group (Scheme 5). In addition, these five-membered ring heterocycles allowed us to maintain the spatial relationship between the adamantyl, indole, and the 3,5-dicarboxyanilide moieties present in the pharmacophore of compound **5**.

A single amide was included so that the negative field point generated by its carbonyl oxygen could be used to

Scheme 6. Design of Prototype Pyrrole **22** Based on the Indole Pharmacophore **5**^a

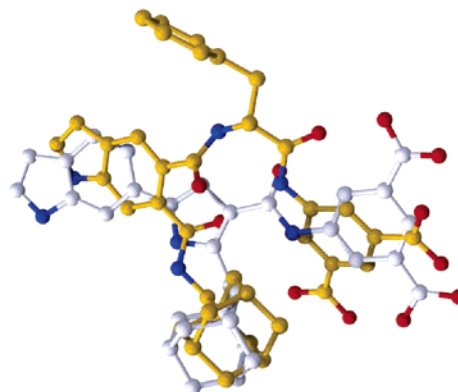


^a The design process involved removal of the benzyl side chain of the Phe residue in indole **5** (gray) and replacement of the two amide groups highlighted (black box) with a pyrrole to give compound **22**. The indole, adamantane, and 3,5-dicarboxyanilide groups were all thought to be essential for activity and were retained in the initial structure.

reinforce that from one of the acid carbonyls. This recreates the pattern of negative points observed around the 3,5-dicarboxyanilide of the pharmacophore, which we considered to be essential for the high levels of *in vitro* activity because we had already shown that removal of one of the carboxylic acids in the indole series had led to a reduction in CCK₂ activity.⁴ In field point terms, removing either of the acids changed the pattern significantly because of the propensity for the amide and carboxylic acid substituents to sit anti to each other, presumably as a result of dipole–dipole repulsion between the two groups.

A model of a prototypical pyrrole (**22**) (Scheme 6) was constructed and subjected to a full conformational hunt. All 42 conformations whose energies lay within 3 kcal/mol of the calculated global minimum were then equipped with field points and compared to those of the pharmacophore shown in Scheme 4. The best 50 overlays were then assessed on the basis of both their electrostatic and steric elements. These could be classified into three broad groups. The results of this experiment showed that there were a small number of overlays (10%) in which the common adamantyl, indole, and 3,5-dicarboxyanilide groups of the two molecules were structurally superimposed (Scheme 7). In fact, the 3,5-dicarboxyanilides were superimposed in all overlays. However, either the indole or adamantane groups of pyrrole **22** were located over the phenylalanine residue of indole **5** in the remainder (data not shown). Nevertheless, the desired superposition (Scheme 7) had been achieved in an albeit small proportion of the overlays examined. Unfortunately, synthesis of the 5-indolylpyrrole **22** first proposed was not possible using the general route described, although the cycloheptyl analogue of the equivalent imidazole (**17g**) was accessible. The affinity of this compound was greatly reduced from that

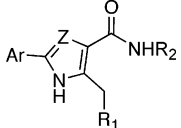
Scheme 7. Overlaying the Field Point Pattern of the CCK₂ Receptor Pharmacophore^a



^a Based on indole **5** (shown in yellow), with a 3 kcal/mol energy range of conformations calculated for the prototype pyrrole **22** (shown in white). The indole, 3,5-dicarboxyanilide, and adamantyl groups are mapped directly over one another in 10% of the overlays stored.

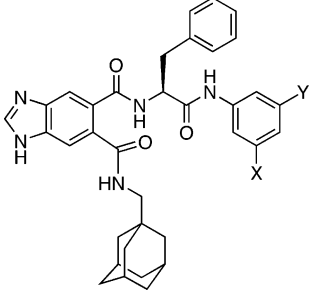
of indole **5** ($pK_i = 6.0 \pm 0.1$), and the reasons for this are not clear. Comparing the two molecules (**17g** and **5**) on the basis of their field point patterns gave the same results as those noted above. Hence, the paucity of “good” overlays, analogous to those in Scheme 7, must suggest that the alternative orientations identified are not tolerated by the receptor binding site. In fact, replacing the pendent indole of **22** with a phenyl group (**10a**) gave a higher level of structural congruence with the desired elements of the pharmacophore (30% of overlays), and these were the first examples to be synthesized. Therefore, this initial example **10a** ($pK_i = 6.9 \pm 0.1$, Table 3) and the close relatives (**10b,c**) are analogues of the phthalate **4** ($pK_i = 7.5 \pm 0.3$, Table 1) rather than indole **5**. These compounds show similar affinities for the CCK₂ receptor, and so the difference is not as great as might appear at first sight. The molecular weights of these compounds were now close to the threshold value of 500 for biliary elimination in man. We were pleased to see that the levels of CCK₁ activity were also broadly similar to those of phthalate **4** and hence that the selectivity for CCK₂ over CCK₁ receptors was maintained. This demonstrated that the field point methodology could be used to design drug candidates with reasonable accuracy, and synthesis of further examples of both pyrrole and imidazole prototypes was begun.

A number of compounds were made in parallel in order to assess differences between the pyrrole (**10a–e**) and imidazole (**17a–e**) series. Modifying the sizes of the 2-aryl and 5-cycloalkylmethyl groups did not increase levels of biological activity, which were consistently robust in both receptor bioassays (Table 3). A single example of a pyrrole with an aliphatic rather than aromatic acid at the 4-position (**10f**) showed a 25-fold decrease in CCK₂ activity. We would attribute this to its failure to maintain the relationship between the acid and adamantyl groups observed in the indole pharmacophore due to the increased flexibility of the linking group between the acid and amide. Most noticeably, the pK_i results obtained for any particular pair of pyrroles and imidazoles were not significantly different in most cases. The largest difference was observed for **10c** and

Table 3. Comparison of Parallel Series of Pyrrole and Imidazole CCK₂ Receptor Antagonists


compd	Z	Ar	R ₁	R ₂	CCK ₂ ^a pK _i ± SEM	CCK ₁ ^a pK _i ± SEM
10a	CH	C ₆ H ₅	1-Ad	3,5-(CO ₂ H) ₂ C ₆ H ₃	6.9 ± 0.1	5.1 ± 0.1
10b	CH	C ₆ H ₅	<i>c</i> -C ₇ H ₁₃	3,5-(CO ₂ H) ₂ C ₆ H ₃	6.6 ± 0.1	5.1 ± 0.1
10c	CH	C ₆ H ₅	1-AdCH ₂	3,5-(CO ₂ H) ₂ C ₆ H ₃	6.7 ± 0.1	5.3 ± 0.1
10d	CH	2-C ₁₀ H ₇	<i>c</i> -C ₇ H ₁₃	3,5-(CO ₂ H) ₂ C ₆ H ₃	6.7 ± 0.1	5.6 ± 0.1
10e	CH	2-C ₁₀ H ₇	<i>c</i> -C ₇ H ₁₃	3-(CO ₂ H)C ₆ H ₄	5.9 ± 0.1	5.4 ± 0.1
10f	CH	C ₆ H ₅	1-Ad	(CH ₂) ₂ CO ₂ H	5.5 ± 0.1	5.0 ± 0.1
17a	N	C ₆ H ₅	1-Ad	3,5-(CO ₂ H) ₂ C ₆ H ₃	6.8 ± 0.1	5.5 ± 0.1
17b	N	C ₆ H ₅	<i>c</i> -C ₇ H ₁₃	3,5-(CO ₂ H) ₂ C ₆ H ₃	6.0 ± 0.1	5.1 ± 0.1
17c	N	C ₆ H ₅	1-AdCH ₂	3,5-(CO ₂ H) ₂ C ₆ H ₃	6.2 ± 0.1	5.2 ± 0.1
17d	N	2-C ₁₀ H ₇	<i>c</i> -C ₇ H ₁₃	3,5-(CO ₂ H) ₂ C ₆ H ₃	6.6 ± 0.1	5.5 ± 0.1
17e	N	2-C ₁₀ H ₇	<i>c</i> -C ₇ H ₁₃	3-(CO ₂ H)C ₆ H ₄	6.1 ± 0.1	5.6 ± 0.1
17f	N	2-C ₁₀ H ₇	<i>c</i> -C ₇ H ₁₃	3,5-(CH ₂ OH) ₂ C ₆ H ₃	5.4 ± 0.1	5.5 ± 0.1
17g	N	5-indolyl	<i>c</i> -C ₇ H ₁₃	3,5-(CO ₂ H) ₂ C ₆ H ₃	6.0 ± 0.1	5.3 ± 0.1

^a Compounds were tested as the bis(*N*-methyl-*D*-glucamine) salts.

Table 4. Effect of Modifying the Aniline Substituent of Benzimidazole Bis-amide CCK₂ Antagonists on Biliary Elimination


compd	X	Y	CCK ₂ ^a pK _i ± SEM	CCK ₁ ^a pK _i ± SEM	MW	log <i>P</i> ^b	% material excreted unchanged ^c
18	CO ₂ H	CO ₂ H	8.3 ± 0.1	5.8 ± 0.3	664	-2.3	45
23	CO ₂ H	H	6.4 ± 0.1	5.3 ± 0.1	620	1.1	39
24	CH ₂ OH	CH ₂ OH	6.2 ± 0.1	5.4 ± 0.1	638	3.7	22

^a Compounds were tested as the bis(*N*-methyl-*D*-glucamine) salts. ^b log *P* measured in octanol/buffer (pH 7.5). ^c % unchanged compound detected in the bile by HPLC following iv bolus administration of the compound at either 1 or 10 μmol/kg to anesthetized rats. The bile duct was cannulated and bile collected over 15 min intervals for a total of 150 min in each case.

17c where this was 0.5 log units. At this stage, these results supported our original proposal that pyrrole and imidazole could be used interchangeably.

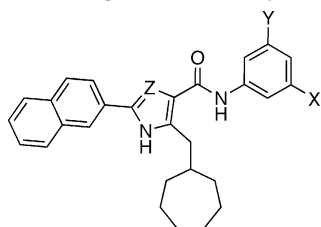
In view of the radical change in structure in moving from the original series, typified by indole **5**, to these new pyrroles and imidazoles, we have assessed a number of compounds for their ability to behave as agonists or antagonists at the CCK₂ receptor. Representative examples, **10a** and **17c**, were tested in the isolated, lumen-perfused immature rat stomach assay.⁴⁶ This is an in vitro assay in which the ability of compounds to cause acid secretion, or block the actions of the full agonist *t*Boc-CCK(29–33) (a small fragment of the hormone CCK), can be examined. In both cases the compounds behaved as simple competitive antagonists and no agonist response was observed. The pK_B values for the two compounds were 6.3 ± 0.4 (**10a**) and 5.6 ± 0.4 (**17c**), in broad agreement with their pK_i values obtained in the CCK₂ receptor radioligand binding assay (Table 3). Therefore, our scaffold-hopping approach has not altered this particular property of the original series.

Biliary Elimination of Pyrroles and Imidazoles.

We were aware that levels of biliary elimination were

particularly high for the original series of indoles and benzimidazoles, to the extent that 45% of the benzimidazole **18** was excreted unchanged in the bile of anesthetized rat (Table 4). This value fell slightly as the polarity of the aniline substituents was reduced by removing one of the carboxylic acids (**23**), a change that was also reflected as an increase in log *P*. However, following this trend further by replacing both of the carboxylic acids by hydroxymethyl groups in the equivalent positions (**24**) failed to reduce excretion below 22% and also resulted in a 100-fold loss of activity for the CCK₂ receptor.

Early examples of the pyrrole series (**10d** and **10e**) were examined in the same model to see whether the reduction in molecular weight had reduced biliary excretion. The compounds were selected on the basis that their in vitro activity was typical of the series and that the molecules contained a naphthalene chromophore, improving their detection by UV-visible spectroscopy relative to the 2-phenyl series. We were disappointed to find that the reduction in molecular weight alone for the diacids did not reduce biliary elimination because 59% of the compound was excreted unchanged by this route (Table 5) with respect to the

Table 5. Effect of Modifying the Aniline Substituent of Pyrrole and Imidazole CCK₂ Antagonists on Biliary Elimination

compd	Z	X	Y	MW	log P ^a	% material excreted unchanged ^b
10d	CH	CO ₂ H	CO ₂ H	511	1.4	59
10e	CH	CO ₂ H	H	467	2.9	6
17d	N	CO ₂ H	CO ₂ H	512	0.7	53
17e	N	CO ₂ H	H	468	2.8	5
17f	N	CH ₂ OH	CH ₂ OH	484	>4	1

^a Measured in octanol/buffer (pH 7.5). ^b % unchanged compound detected in the bile by HPLC following iv bolus administration of the compound at 10 μmol/kg to anesthetized rats. The bile duct was cannulated and bile collected over 15 min intervals for a total of 150 min in each case.

benzimidazoles (Table 4). However, we were delighted to find that significant improvements were observed in the case of the pyrrole monoacid (**10e**) such that levels of biliary excretion were now reduced to 6%. Furthermore, the loss of in vitro activity engendered by this change was less than 10-fold compared to a loss of almost 100-fold for the same change in the benzimidazole series (**18–23**). The same pattern of behavior was found for the equivalent imidazoles where removal of one of the carboxylic acids reduced elimination from 53% for the diacid **17d** to 5% for the monoacid **17e**. Further modification of the two aniline substituents to hydroxymethyl groups (**17f**) reduced this further to 1%. This suggests that the changes in polarity of the aniline substituent are important in determining the degree to which a compound is susceptible to biliary elimination but that their significance is greater for these lower molecular weight compounds. While the small additional loss of in vitro activity detracted from this favorable result, the 3-substituted monoacids, **10e** and **17e**, were nonetheless our preferred choice as lead compounds for the development of this class of CCK₂ antagonists. The results of these studies will be described in the accompanying paper.⁴⁹

Conclusion

We have demonstrated that field points can be used as simple descriptors of molecular properties. This approach has been successfully applied to the design of a novel series of CCK₂ antagonists in a process of "scaffold hopping" from a known series of indoles with high in vitro affinity and selectivity but poor bioavailability. We intend to develop this molecular modeling technique further because we believe that it represents a simple way of comparing molecules on the basis of their electrostatic and van der Waals properties rather than their structural frameworks. The structural diversity of the compounds used as input for creation of the pharmacophore was deliberately conservative because this allowed us to evaluate the results from the field point overlays easily. However, since this method

does not rely on relating common structural motifs, it should also be applicable to the wide range of compounds that have also been described as CCK₂ receptor antagonists in recent years,¹⁰ and future investigations will be directed toward this end.

The new series of pyrroles and imidazoles are not as potent as the original indoles in vitro but have greater potential as drug candidates in terms of their reduced tendency to biliary excretion. This makes them good lead compounds for development of a new series whose base structures are not obviously related to those of the parent compounds. We have also demonstrated that the reduction of molecular weight from 664 (**18**) to 511 (**10d**) is not sufficient in itself to prevent biliary elimination; indeed, this rose by 10% in the first examples examined. However, a concomitant reduction in the polarity of both the pyrrole and imidazole series, obtained by modification of the aniline substituents, produced a significant reduction in biliary elimination when compared to an equivalent series of benzimidazoles and gave us two new series of lead compounds. We have gone on to develop the imidazole series into compounds with nanomolar affinity and high bioavailability in vivo, and this work is described elsewhere.⁴⁹

Experimental Section

Abbreviations. 1-Ad, adamantan-1-yl; EDC, 1-(3-dimethylaminopropyl)-3-ethylcarbodiimide hydrochloride; DMAP, 4-(dimethylamino)pyridine; HOBt, 1-hydroxybenzotriazole; OXONE, potassium hydrogen peroxymonosulfate sulfate (2KHSO₅·KHSO₄·K₂SO₄, 5:3:2:2, CAS registry no. 70693-62-8).

General. NMR spectra were recorded on a Bruker DRX 300 spectrometer with chemical shifts reported in ppm relative to tetramethylsilane used as internal standard. Elemental analyses were determined at the London School of Pharmacy and are within 0.4% of the theoretical values. Merck silica gel 60 (40–63 μm) was used for column chromatography.

3-Adamantan-1-ylpropionic acid was prepared from 1-bromoadamantane,⁵⁰ and cycloheptylacetic acid was obtained from cycloheptanone.⁵¹ The aniline derivatives **9a** and **9b** were prepared from the relevant nitrobenzoic acids, while **9c** was synthesized from 5-nitro-*m*-xylene- α,α' -diol.

The 1H-pyrrole-3-carboxylic acid intermediates **8a–d** were prepared by the method described below.

2-Adamantan-1-ylmethyl-5-phenyl-1H-pyrrole-3-carboxylic Acid (8a). Step a. To a solution of 4-adamantan-1-yl-3-oxobutyric acid ethyl ester³⁷ (3.00 g, 11.0 mmol) in acetone (30 mL) was added sodium iodide (0.55 g, 3.67 mmol) and anhydrous potassium carbonate (3.04 g, 22.0 mmol), followed by a solution of 2-bromo-1-phenylethanone (2.38 g, 11.5 mmol) in acetone (10 mL). The mixture was heated at reflux for 36 h, cooled to room temperature, and filtered. The filtrate was evaporated, and the residue was dissolved in diethyl ether (50 mL) and washed with H₂O (2 × 20 mL). The organic phase was dried (MgSO₄), and the solvent was evaporated. The residue was purified by chromatography on silica gel using hexanes–EtOAc (4:1) as eluant to afford 4-adamantan-1-yl-3-oxo-2-(2-oxo-2-phenylethyl)butyric acid ethyl ester as a pale-yellow oil (1.92 g, 46%). ¹H NMR (CDCl₃) δ 7.98 (2H, m), 7.65 (1H, m), 7.46 (2H, m), 5.59 (1H, m), 4.19 (3H, m), 3.60 (2H, dd, *J* = 7.2, 17.1 Hz), 2.50 (2H, m), 1.96 (3H, br s), 1.68 (12H, m), 1.29 (3H, t, *J* = 7.2 Hz).

Step b. 4-Adamantan-1-yl-3-oxo-2-(2-oxo-2-phenylethyl)butyric acid ethyl ester (1.10 g, 2.88 mmol) and ammonium acetate (780 mg, 10.1 mmol) were stirred in acetic acid (1.4 mL) at 80 °C for 24 h. The reaction mixture was cooled, then partitioned between CH₂Cl₂ (50 mL) and saturated aqueous NaHCO₃ (50 mL). The organic layer was dried over Na₂SO₄, and the solvent was evaporated. The residue was crystallized

from hexanes–EtOAc (4:1) to afford 2-adamantan-1-ylmethyl-5-phenyl-1*H*-pyrrole-3-carboxylic acid ethyl ester (**7a**) as a white solid (750 mg, 71%). ¹H NMR (CDCl₃) δ 8.21 (1H, br s), 7.48–7.21 (5H, m), 6.88 (1H, d, *J* = 2.7 Hz), 4.30 (2H, q, *J* = 7.0 Hz), 2.85 (2H, s), 1.96 (3H, br s), 1.60 (12H, m), 1.38 (3H, t, *J* = 7.0 Hz).

Step c. To a solution of **7a** (750 mg, 2.06 mmol) in EtOH (45 mL) was added 6 M sodium hydroxide (5 mL). The mixture was heated at reflux for 48 h, allowed to cool to room temperature, and concentrated to a small volume under reduced pressure. The concentrated solution was diluted with 2 M HCl (40 mL), the precipitated solid was filtered, washed with H₂O, and dried to afford **8a** (660 mg, 94%). ¹H NMR (CDCl₃) δ 11.5 (1H, br s), 8.26 (1H, br s), 7.48 (2H, m), 7.40 (2H, m), 7.26 (1H, m), 6.94 (1H, d, *J* = 3.0 Hz), 2.87 (2H, s), 1.97 (3H, br s), 1.63 (12H, m).

5-[(2-Adamantan-1-ylmethyl-5-phenyl-1*H*-pyrrole-3-carbonyl)amino]isophthalic Acid (10a**).** **Step d.** To a suspension of **8a** (290 mg, 0.91 mmol) in CH₂Cl₂ (5 mL) was added thionyl chloride (200 μL, 2.74 mmol) and 1 drop of DMF. The mixture was stirred at room temperature for 30 min, and the solvent was evaporated. Any remaining DMF was removed by coevaporation with a further two portions of CH₂Cl₂ (5 mL). 5-Aminoisophthalic acid dibenzyl ester (**9a**) (361 mg, 1.00 mmol) and anhydrous pyridine (2 mL) were then added to the residue. The solution was kept at room temperature for 16 h and diluted with CH₂Cl₂ (30 mL). The organic phase was washed with 2 M HCl (2 × 20 mL), brine (20 mL), and dried (MgSO₄), and the solvent was evaporated. The residue was purified by chromatography on silica gel using CH₂Cl₂–hexanes–EtOAc (9:9:2) as eluant to afford 5-[(2-adamantan-1-ylmethyl-5-phenyl-1*H*-pyrrole-3-carbonyl)amino]isophthalic acid dibenzyl ester as a pale-yellow solid (300 mg, 45%). ¹H NMR (CDCl₃) δ 8.48 (3H, s), 8.30 (1H, br s), 7.69 (1H, s), 7.49–7.27 (15H, m), 6.66 (1H, d, *J* = 2.7 Hz), 5.40 (4H, s), 2.91 (2H, s), 1.95 (3H, br s), 1.63 (12H, m).

Step e. A round-bottom flask containing 5-[(2-adamantan-1-ylmethyl-5-phenyl-1*H*-pyrrole-3-carbonyl)amino]isophthalic acid dibenzyl ester (180 mg, 0.27 mmol), 10% palladium on charcoal (50 mg), and THF–MeOH (1:1 mixture, 20 mL) was evacuated and flushed with hydrogen three times. The mixture was vigorously stirred overnight under an atmosphere of hydrogen. The catalyst was removed by filtration and the filtrate was evaporated to afford **10a** as a white solid (130 mg, 98%). ¹H NMR (DMSO-*d*₆) δ 13.17 (2H, br s), 11.22 (1H, s), 9.80 (1H, s), 8.64 (2H, s), 8.13 (1H, s), 7.66 (2H, m), 7.39 (2H, m), 7.19 (2H, m), 2.85 (2H, s), 1.88 (3H, br s), 1.53 (12H, m). It was further characterized as the di(*N*-methyl-*D*-glucamine) salt (fluffy white solid). Anal. (C₃₀H₃₀N₂O₅·2C₇H₁₇NO₅·2.0H₂O) C, H, N.

Compounds **10b–d** were prepared by a similar sequence for **8b–d**. **10e** was prepared from **8d** by a similar sequence used to obtain **10a** except that 3-aminobenzoic acid benzyl ester (**9b**) was used in place of 5-aminoisophthalic acid dibenzyl ester (**9a**) in step d. **10f** was prepared from **8a** by a similar sequence used to obtain **10a** except that β-alanine benzyl ester was used in place of 5-aminoisophthalic acid dibenzyl ester in step d.

5-[(2-Cycloheptylmethyl-5-phenyl-1*H*-pyrrole-3-carbonyl)amino]isophthalic Acid (10b**).** ¹H NMR (DMSO-*d*₆) further characterized the product as the di(*N*-methyl-*D*-glucamine) salt (fluffy white solid). Anal. (C₂₇H₂₈N₂O₅·2C₇H₁₇NO₅·2.0H₂O) C, H, N.

5-[(2-Adamantan-1-ylethyl)-5-phenyl-1*H*-pyrrole-3-carbonyl]amino]isophthalic Acid (10c**).** ¹H NMR (DMSO-*d*₆) further characterized the product as the di(*N*-methyl-*D*-glucamine) salt (fluffy white solid). Anal. (C₃₁H₃₂N₂O₅·2C₇H₁₇NO₅·3.0H₂O) C, H, N.

5-(2-Cycloheptylmethyl-5-naphthalene-2-yl-1*H*-pyrrole-3-carbonyl)amino]isophthalic Acid (10d**).** ¹H NMR (DMSO-*d*₆) further characterized the product as the di(*N*-methyl-*D*-glucamine) salt (fluffy white solid). Anal. (C₃₁H₃₀N₂O₅·2C₇H₁₇NO₅·3.0H₂O) C, H, N.

3-[(2-Cycloheptylmethyl-5-naphthalene-2-yl-1*H*-pyrrole-3-carbonyl)amino]Benzoic Acid (10e**).** ¹H NMR (DMSO-

*d*₆) further characterized the product as the *N*-methyl-*D*-glucamine salt (fluffy white solid). Anal. (C₃₀H₃₀N₂O₃·C₇H₁₇NO₅·2.5H₂O) C, H, N.

3-[(2-Adamantan-1-ylmethyl-5-phenyl-1*H*-pyrrole-3-carbonyl)amino]propionic Acid (10f**).** ¹H NMR (DMSO-*d*₆) further characterized the product as the *N*-methyl-*D*-glucamine salt (fluffy white solid). Anal. (C₂₅H₃₀N₂O₃·C₇H₁₇NO₅·H₂O) C, H, N.

The 1*H*-imidazole-4-carboxylic acid intermediates **15a–d** were prepared by the representative method described below (Scheme 2).

5-Cycloheptylmethyl-2-naphthalen-2-yl-1*H*-imidazole-4-carboxylic Acid (15d**).** **Step a.** To a solution of cycloheptylacetic acid (10.0 g, 64.0 mmol) and (carbethoxymethylene)-triphenylphosphorane (22.4 g, 64.0 mmol) in CH₂Cl₂ (250 mL) were added EDC (12.25 g, 64.0 mmol) and DMAP (cat.) at 0 °C. The solution was stirred at this temperature for 1 h, then at room temperature for 16 h. The reaction mixture was washed with saturated aqueous NaHCO₃ (2 × 100 mL) and dried (MgSO₄). Filtration and evaporation of the solvent gave the crude product, which crystallized from EtOAc to afford 4-cycloheptyl-3-oxo-2-(triphenyl-λ⁵-phosphanylidenebutyric acid ethyl ester (23.6 g, 76%). ¹H NMR (CDCl₃) δ 7.68–7.27 (15H, m), 3.73 (2H, m), 2.77 (2H, d, *J* = 6.9 Hz), 2.07 (1H, m), 1.73–1.41 (10H, m), 1.22 (2H, m), 0.67 (3H, m).

Step b. To a solution of 4-cycloheptyl-3-oxo-2-(triphenyl-λ⁵-phosphanylidenebutyric acid ethyl ester (12.1 g, 25.0 mmol) in THF (200 mL) and H₂O (100 mL) was added OXONE (23.0 g, 37.5 mmol) at 0 °C. The solution was stirred at room temperature for 16 h and diluted with H₂O (300 mL), and the product was extracted with EtOAc (2 × 150 mL). The organic phase was dried and filtered, and the solvent was evaporated. The crude product was purified by chromatography on silica gel using CH₂Cl₂–EtOAc (9:1) as eluant, affording 4-cycloheptyl-2,3-dioxobutyric acid ethyl ester hydrate as a pale-yellow oil (5.70 g, 88%). ¹H NMR (CDCl₃) δ 4.99 (2H, br s), 4.30 (2H, q, *J* = 6.9 Hz), 2.51 (2H, d, *J* = 6.9 Hz), 2.14 (1H, m), 1.67–1.16 (15H, m).

Step c. To a slurry of ammonium acetate (9.0 g, 116.0 mmol) in acetic acid (35 mL) was added 4-cycloheptyl-2,3-dioxobutyric acid ethyl ester hydrate (3.0 g, 11.6 mmol) followed by 2-naphthaldehyde (3.6 g, 23.2 mmol). The mixture was stirred in an oil bath heated to 70 °C for 2 h. The solution was cooled to room temperature, and the acetic acid was evaporated. The residue was dissolved in EtOAc (50 mL) and washed with saturated aqueous NaHCO₃ (2 × 50 mL), H₂O (20 mL), and brine (20 mL). The organic phase was dried (MgSO₄), and the solvent was evaporated. The crude product was purified by crystallization from EtOAc to afford 5-cycloheptylmethyl-2-naphthalen-2-yl-1*H*-imidazole-4-carboxylic acid ethyl ester (**14d**) as a white solid (1.74 g, 40%). ¹H NMR (CDCl₃) δ 10.18 and 9.97 (1H, br s), 8.39 (1H, s), 7.90 (4H, m), 7.52 (2H, br s), 4.40 (2H, q, *J* = 9.0 Hz), 2.89 (2H, m), 2.05–1.26 (16H, m).

Step d. To a suspension of **14d** (1.73 g, 4.62 mmol) in EtOH (25 mL) was added a solution of sodium hydroxide (1.29 g, 32.3 mmol) in H₂O (5 mL). The reaction mixture was heated under reflux for 48 h, allowed to cool to room temperature, and concentrated under reduced pressure. The aqueous solution was diluted with H₂O (30 mL) and acidified to pH 2 with 1 M HCl. The precipitate was collected by filtration, washed with H₂O, and dried to afford **15d** as an off-white solid (1.53 g, 96%). ¹H NMR (DMSO-*d*₆) δ 8.77 (1H, s), 8.24–7.98 (4H, m), 7.64 (2H, m), 2.91 (1H, d, *J* = 6.9 Hz), 2.64 (1H, d, *J* = 6.9 Hz), 2.03 (1H, m), 1.69–1.24 (12H, m).

5-[(5-Cycloheptylmethyl-2-naphthalen-2-yl-1*H*-imidazole-4-carbonyl)amino]isophthalic Acid (17d**).** **Step e.** To a solution of **15d** (500 mg, 1.44 mmol) and 5-aminoisophthalic acid dibenzyl ester (**9a**) (520 mg, 1.44 mmol) in DMF (3 mL) were added HOBt (195 mg, 1.44 mmol), DMAP (cat.), and EDC (280 mg, 1.44 mmol). The solution was kept at room temperature for 72 h and poured over 1 M HCl (20 mL), and the product was extracted with EtOAc (2 × 20 mL). The product crystallized from the EtOAc extracts. The crystals were collected by filtration, dried, and washed with MeOH to afford

5-[(5-cycloheptylmethyl-2-naphthalen-2-yl-1*H*-imidazole-4-carbonyl)amino]isophthalic acid dibenzyl ester (**16d**) as a white solid (453 mg, 46%). ¹H NMR (DMSO-*d*₆) δ 13.00 (1H, br s), 10.50 (1H, s), 8.84 (2H, s), 8.61 (1H, s), 8.28 (2H, m), 8.00 (3H, m), 7.50 (12H, m), 5.41 (4H, s), 2.98 (2H, d, *J* = 6.0 Hz), 2.00 (1H, m), 1.69–1.16 (12H, m).

Step f. 16d (450 mg, 0.65 mmol) was deprotected using the same procedure as in step e in the preparation of **10a** to afford **17d** as white solid (310 mg, 94%). ¹H NMR (DMSO-*d*₆) δ 10.75 (1H, s), 8.77 (3H, m), 8.40 (1H, d, *J* = 6.0 Hz), 8.25 (1H, s), 8.13 (1H, d, *J* = 6.0 Hz), 8.02 (2H, m), 7.65 (2H, m), 3.05 (2H, d, *J* = 9.0 Hz), 2.11 (1H, m), 1.75–1.31 (12H, m). The product was further characterized as the di(*N*-methyl-*D*-glucamine) salt (fluffy white solid). Anal. (C₃₀H₂₉N₃O₅·2C₇H₁₇NO₅·4.8H₂O) C, H, N.

17a–c were prepared by a similar sequence from the carboxylic acid intermediates **15a–c**, respectively.

5-[(5-Adamantan-1-ylmethyl-2-phenyl-1*H*-imidazole-4-carbonyl)amino]isophthalic Acid (17a). ¹H NMR (DMSO-*d*₆) further characterized the product as the di(*N*-methyl-*D*-glucamine) salt (fluffy white solid). Anal. (C₂₉H₂₉N₃O₅·2C₇H₁₇NO₅·0.4H₂O) C, H, N.

5-[(5-Cycloheptylmethyl-2-phenyl-1*H*-imidazole-4-carbonyl)amino]isophthalic Acid (17b). ¹H NMR (DMSO-*d*₆) further characterized the product as the di(*N*-methyl-*D*-glucamine) salt (fluffy white solid). Anal. (C₂₆H₂₇N₃O₅·2C₇H₁₇NO₅·2.4H₂O) C, H, N.

5-[(5-(2-Adamantan-1-ylethyl)-2-phenyl-1*H*-imidazole-4-carbonyl)amino]isophthalic Acid (17c). ¹H NMR (DMSO-*d*₆) further characterized the product as the di(*N*-methyl-*D*-glucamine) salt (fluffy white solid). Anal. (C₃₀H₃₁N₃O₅·2C₇H₁₇NO₅·6.2H₂O) C, H, N.

3-[(5-Cycloheptylmethyl-2-naphthalen-2-yl-1*H*-imidazole-4-carbonyl)amino]benzoic Acid (17e). **17e** was prepared from **15d** by a similar sequence used to obtain **17d** except that 3-aminobenzoic acid benzyl ester (**9b**) was used in place of 5-aminoisophthalic acid dibenzyl ester (**9a**) in step d. ¹H NMR (DMSO-*d*₆) further the product characterized as the *N*-methyl-*D*-glucamine salt (fluffy white solid). Anal. (C₂₉H₂₉N₃O₅·C₇H₁₇NO₅·4.8H₂O) C, H, N.

5-Cycloheptylmethyl-2-naphthalen-2-yl-1*H*-imidazole-4-carboxylic Acid (3,5-Bis-hydroxymethylphenyl)amide (17f). **17f** was prepared from **15d** and **9c** according to step d, and the intermediate **16f** was deprotected according to the procedure of step g.

5-Cycloheptylmethyl-2-naphthalen-2-yl-1*H*-imidazole-4-carboxylic acid (3,5-(dimethoxycarbonyloxymethyl)phenyl)amide (**16f**) was obtained according to step e in the sequence used for the preparation of **17d** except that 3,5-dimethoxycarbonyloxymethylaniline (**9c**) was used in place of 5-aminoisophthalic acid dibenzyl ester (**9a**).

Step g. To a solution of **16f** (438 mg, 0.72 mmol) in MeOH (50 mL) was slowly added a 1% aqueous solution of potassium carbonate. The mixture was stirred at room temperature for 2 h, then heated at reflux for 1 h. The reaction mixture was allowed to cool to room temperature, and the MeOH was evaporated. The precipitate was collected by filtration, washed with H₂O, and dried to afford **17f** as a white solid (290 mg, 83%). ¹H NMR (DMSO-*d*₆) experiments were conducted. Anal. (C₃₀H₃₃N₃O₃) C, H, N.

5-[(5-Cycloheptylmethyl-2-(1*H*-indol-5-yl)-1*H*-imidazole-4-carbonyl)amino]isophthalic Acid (17g). **17g** was prepared by a sequence similar to the preparation of **17d** from **15e**. ¹H NMR (DMSO-*d*₆) further characterized the product as the di(*N*-methyl-*D*-glucamine) salt (fluffy white solid). Anal. (C₂₈H₂₈N₄O₅·2C₇H₁₇NO₅·3.0H₂O) C, H, N.

Acknowledgment. We thank Dr. Elaine Harper and Mr. Eric Griffin for providing the radioligand binding data and Dr. David Neuhaus, of the MRC Laboratory of Molecular Biology, Cambridge, U.K., for his assistance with the NMR experiments described.

Supporting Information Available: Analytical data for compounds used in biological tests. This material is available free of charge via the Internet at <http://pubs.acs.org>.

References

- Black, J. W.; Kalindjian, S. B. Gastrin agonists and antagonists. *Pharmacol. Toxicol.* **2002**, *91*, 275–281.
- Kalindjian, S. B.; Bodkin, M. J.; Buck, I. M.; Dunstone, D. J.; Low, C. M. R.; McDonald, I. M.; Pether, M. J.; Steel, K. I. M. A new class of nonpeptidic cholecystokinin-B gastrin receptor antagonists based on dibenzobicyclo[2.2.2]octane. *J. Med. Chem.* **1994**, *37*, 3671–3673.
- Kalindjian, S. B.; Buck, I. M.; Cushnir, J. R.; Dunstone, D. J.; Hudson, M. L.; Low, C. M.; McDonald, I. M.; Pether, M. J.; Steel, K. I.; Tozer, M. J. Improving the affinity and selectivity of a nonpeptide series of cholecystokinin-B/gastrin receptor antagonists based on the dibenzobicyclo[2.2.2]octane skeleton. *J. Med. Chem.* **1995**, *38*, 4294–4302.
- Kalindjian, S. B.; Buck, I. M.; Davies, J. M.; Dunstone, D. J.; Hudson, M. L.; Low, C. M.; McDonald, I. M.; Pether, M. J.; Steel, K. I.; Tozer, M. J.; Vinter, J. G. Non-peptide cholecystokinin-B/gastrin receptor antagonists based on bicyclic, heteroaromatic skeletons. *J. Med. Chem.* **1996**, *39*, 1806–1815.
- McDonald, I. M.; Dunstone, D. J.; Kalindjian, S. B.; Linney, I. D.; Low, C. M.; Pether, M. J.; Steel, K. I.; Tozer, M. J.; Vinter, J. G. 2,7-Dioxo-2,3,4,5,6,7-hexahydro-1*H*-benzo[*h*][1,4]diazonine as a new template for the design of CCK(2) receptor antagonists. *J. Med. Chem.* **2000**, *43*, 3518–3529.
- Jensen, R. T. Involvement of cholecystokinin/gastrin-related peptides and their receptors in clinical gastrointestinal disorders. *Pharmacol. Toxicol.* **2002**, *91*, 333–350.
- Noble, F.; Roques, B. P. CCK-B receptor: chemistry, molecular biology, biochemistry and pharmacology. *Prog. Neurobiol.* **1999**, *58*, 349–379.
- Wank, S. A. G protein-coupled receptors in gastrointestinal physiology. I. CCK receptors: an exemplary family. *Am. J. Physiol.* **1998**, *274*, G607–G613.
- Steel, K. Gastrin and gastrin receptor ligands. A review of recent patent literature. *IDrugs* **2002**, *5*, 689–695.
- McDonald, I. M. CCK2 receptor antagonists. *Expert Opin. Ther. Pat.* **2001**, *11*, 445–462.
- Hill, D. R.; Shaw, T. M.; Graham, W.; Woodruff, G. N. Autoradiographical detection of cholecystokinin-A receptors in primate brain using ¹²⁵I-Bolton Hunter CCK8 and ³H-MK-329. *J. Neurosci.* **1990**, *10*, 1070–1081.
- Jebbink, M. C. W.; Jansen, J. M. B. J.; Mooy, D. M.; Rovati, L. C.; Lamers, C. B. H. W. Effect of the specific cholecystokinin receptor antagonist Loxiglumide on bombesin stimulated pancreatic enzyme secretion in man. *Regul. Pept.* **1991**, *32*, 361–368.
- Douglas, B. R.; Jebbink, M. C.; Tjon a Tham, R. T.; Jansen, J. B.; Lamers, C. B. The effect of loxiglumide (CR-1505) on basal and bombesin-stimulated gallbladder volume in man. *Eur. J. Pharmacol.* **1989**, *166*, 307–309.
- Moran, T. H.; Robinson, P. H.; Goldrich, M. S.; McHugh, P. R. 2 Brain cholecystokinin receptors. Implications for behavioral actions. *Brain Res.* **1986**, *362*, 175–179.
- Lee, Y. M.; Beinborn, M.; McBride, E. W.; Lu, M.; Kolakowski, L. F.; Kopin, A. S. The human brain cholecystokinin-B gastrin receptor. Cloning and characterization. *J. Biol. Chem.* **1993**, *268*, 8164–8169.
- Ulrich, C. D.; Ferber, I.; Holicky, E.; Hadac, E.; Buell, G.; Miller, L. J. Molecular-cloning and functional expression of the human gallbladder cholecystokinin-a receptor. *Biochem. Biophys. Res. Commun.* **1993**, *193*, 204–211.
- Pisegna, J. R.; Deweerth, A.; Huppi, K.; Wank, S. A. Molecular-cloning, functional expression, and chromosomal localization of the human cholecystokinin type-a receptor. *Ann. N. Y. Acad. Sci.* **1994**, *713*, 338–342.
- Deweerth, A.; Pisegna, J. R.; Huppi, K.; Wank, S. A. Molecular-cloning, functional expression and chromosomal localization of the human cholecystokinin type-a receptor. *Biochem. Biophys. Res. Commun.* **1993**, *194*, 811–818.
- Bock, M. G.; DiPardo, R. M.; Evans, B. E.; Rittle, K. E.; Whitter, W. L.; Veber, D. E.; Anderson, P. S.; Freidinger, R. M. Benzodiazepine gastrin and brain cholecystokinin receptor ligands: L-365,260. *J. Med. Chem.* **1989**, *32*, 13–16.
- Simple, G.; Ryder, H.; Rooker, D. P.; Batt, A. R.; Kendrick, D. A.; Szelke, M.; Ohta, M.; Satoh, M.; Nishida, A.; Akuzawa, S.; Miyata, K. (3*R*)-*N*-(1-(*tert*-butylcarbonylmethyl)-2,3-dihydro-2-oxo-5-(2-pyridyl)-1*H*-1,4-benzodiazepin-3-yl)-*N'*-(3-(methylamino)phenyl)urea (YF476): a potent and orally active gastrin/CCK-B antagonist. *J. Med. Chem.* **1997**, *40*, 331–341.

- (21) Horwell, D. C.; Hughes, J.; Hunter, J. C.; Pritchard, M. C.; Richardson, R. S.; Roberts, E.; Woodruff, G. N. Rationally designed "dipeptoid" analogues of CCK. α -Methyltryptophan derivatives as highly selective and orally active gastrin and CCK-B antagonists with potent anxiolytic properties. *J. Med. Chem.* **1991**, *34*, 404–414.
- (22) Goodford, P. J. A computational procedure for determining energetically favorable binding sites on biologically important macromolecules. *J. Med. Chem.* **1985**, *28*, 849–857.
- (23) Klebe, G.; Abraham, U.; Mietzner, T. Molecular similarity indices in a comparative analysis (CoMSIA) of drug molecules to correlate and predict their biological activity. *J. Med. Chem.* **1994**, *37*, 4130–4146.
- (24) Cramer, R.; Patterson, D.; Bruce, J. Comparative molecular field analysis (CoMFA). 1. Effect of shape on binding of steroids to carrier proteins. *J. Am. Chem. Soc.* **1988**, *110*, 5959–5967.
- (25) Vinter, J. G.; Trollope, K. I. Multiconformational composite molecular-potential fields in the analysis of drug-action. 1. Methodology and first evaluation using 5-HT and histamine action as examples. *J. Comput.-Aided Mol. Des.* **1995**, *9*, 297–307.
- (26) Vinter, J. G. Extended electron distributions applied to the molecular mechanics of some intermolecular interactions. *J. Comput.-Aided Mol. Des.* **1994**, *8*, 653–668.
- (27) Hunter, C.; Sanders, J. The nature of π - π interactions. *J. Am. Chem. Soc.* **1990**, *112*, 5525.
- (28) Gundertofte, K.; Liljefors, T.; Norrby, P.-O.; Pettersson, I. A comparison of conformational energies calculated by several molecular mechanics methods. *J. Comput. Chem.* **1996**, *17*, 429–449.
- (29) Halgren, T. http://www.ccl.net/ccca/data/ff_evaluation_suite/.
- (30) Chessari, G.; Hunter, C. A.; Low, C. M.; Packer, M. J.; Vinter, J. G.; Zonta, C. An evaluation of force-field treatments of aromatic interactions. *Chemistry* **2002**, *8*, 2860–2867.
- (31) Marshall, G. R.; Cramer, R. D., 3rd. Three-dimensional structure-activity relationships. *Trends Pharmacol. Sci.* **1988**, *9*, 285–289.
- (32) Lemmen, C.; Lengauer, T. Computational methods for the structural alignment of molecules. *J. Comput.-Aided Mol. Des.* **2000**, *14*, 215–232.
- (33) Hann, M. M.; Leach, A. R.; Harper, G. Molecular complexity and its impact on the probability of finding leads for drug discovery. *J. Chem. Inf. Comput. Sci.* **2001**, *41*, 856–864.
- (34) Lange, J. H.; Kruse, C. G. Keynote review: Medicinal chemistry strategies to CB1 cannabinoid receptor antagonists. *Drug Discovery Today* **2005**, *10*, 693–702.
- (35) Lloyd, D. G.; Buenemann, C. L.; Todorov, N. P.; Manallack, D. T.; Dean, P. M. Scaffold hopping in de novo design. Ligand generation in the absence of receptor information. *J. Med. Chem.* **2004**, *47*, 493–496.
- (36) Jenkins, J. L.; Glick, M.; Davies, J. W. A 3D similarity method for scaffold hopping from known drugs or natural ligands to new chemotypes. *J. Med. Chem.* **2004**, *47*, 6144–6159.
- (37) Wierenga, W.; Skulnick, H. I. General, efficient, one-step synthesis of β -keto-esters. *J. Org. Chem.* **1979**, *44*, 310–311.
- (38) Chiu, P. K.; Sammes, M. P. The synthesis and chemistry of azolenines. Part 18. Preparation of 3-ethoxycarbonyl-3H-pyrroles via the Paal-Knorr reaction, and sigmatropic rearrangements involving competitive ester migrations to C-2, C-4 and N. *Tetrahedron* **1990**, *46*, 3439–3456.
- (39) Wasserman, H. H.; Vu, C. B. Formation of vicinal tricarbonyl compounds by selective oxidation of ylides using potassium peroxymonosulfate. *Tetrahedron Lett.* **1990**, *31*, 5205–5308.
- (40) Wasserman, H. H.; Ennis, D. S.; Blum, C. A.; Rotello, V. M. The conversion of carboxylic acids to keto phosphorane precursors of 1,2,3-vicinal tricarbonyl compounds. *Tetrahedron Lett.* **1992**, *33*, 6003–6006.
- (41) Brackeen, M. F.; Stafford, J. A.; Feldman, P. L.; Karanewsky, D. S. An efficient and mild synthesis of highly substituted imidazoles. *Tetrahedron Lett.* **1994**, *35*, 1635–1638.
- (42) XED Software from Cresset BioMolecular Discovery Ltd., Spirella Building, Bridge Road, Letchworth, Herts, SG6 4ET, U.K.
- (43) Goodman, J. M. *Chemical Applications of Molecular Modelling*; Royal Society of Chemistry: Cambridge, U.K., 1998; pp 186–188.
- (44) Harper, E. A.; Roberts, S. P.; Shankley, N. P.; Black, J. W. Analysis of variation in L-365,260 competition curves in radioligand binding assays. *Br. J. Pharmacol.* **1996**, *118*, 1717–1726.
- (45) Hull, R. A. D.; Shankley, N. P.; Harper, E. A.; Gerskowitch, V. P.; Black, J. W. 2-Naphthalenesulphonyl L-aspartyl-(2-phenethyl)amide (2-Nap), a selective cholecystokinin CCK(A)-receptor antagonist. *Br. J. Pharmacol.* **1993**, *108*, 734–740.
- (46) Welsh, N. J.; Shankley, N. P.; Black, J. W. Comparative analysis of the vagal stimulation of gastric acid secretion in rodent isolated stomach preparations. *Br. J. Pharmacol.* **1994**, *112*, 93–96.
- (47) Horwell, D. C.; Beeby, A.; Clark, C. R.; Hughes, J. Synthesis and binding affinities of analogues of cholecystokinin-(30–33) as probes for central nervous system cholecystokinin receptors. *J. Med. Chem.* **1987**, *30*, 729–732.
- (48) Low, C. M.; Black, J. W.; Broughton, H. B.; Buck, I. M.; Davies, J. M.; Dunstone, D. J.; Hull, R. A.; Kalindjian, S. B.; McDonald, I. M.; Pether, M. J.; Shankley, N. P.; Steel, K. I. Development of peptide 3D structure mimetics: rational design of novel peptoid cholecystokinin receptor antagonists. *J. Med. Chem.* **2000**, *43*, 3505–3517.
- (49) Buck, I. M.; Black, J. W.; Cooke, T.; Dunstone, D. J.; Gaffen, J. D.; Griffin, E. P.; Harper, E. A.; Hull, R. A. D.; Kalindjian, S. B.; Lilley, E. J.; Linney, I. D.; Low, C. M. R.; McDonald, I. M.; Pether, M. J.; Roberts, S. P.; Shankley, N. P.; Shaxted, M. E.; Steel, K. I. M.; Sykes, D. A.; Tozer, M. J.; Watt, G. F.; Walker, M. K.; Wright, L.; Wright, P. T. Optimization of the in vitro and in vivo properties of a novel series of 2,4,5-trisubstituted imidazoles as potent cholecystokinin-2 (CCK₂) antagonists. *J. Med. Chem.* **2005**, *48*, 6803–6812.
- (50) Ohno, M.; Ishizaki, K.; Eguchi, S. Synthesis of adamantane derivatives by bridgehead radical addition to electron-deficient unsaturated bonds. *J. Org. Chem.* **1988**, *53*, 1285–1288.
- (51) Yokohama, S.; Miwa, T.; Aibara, S.; Fujiwara, H.; Matsumoto, H.; Nakayama, K.; Iwamoto, T.; Mori, M.; Moroi, R.; Tsukada, W.; et al. Synthesis and anti-allergy activity of [1,3,4]thiadiazolo-[3,2-a]-1,2,3-triazolo[4,5-d]pyrimidin-9(3H)-one derivatives. II. 6-Alkyl- and 6-cycloalkylalkyl derivatives. *Chem. Pharm. Bull. (Tokyo)* **1992**, *40*, 2391–2398.

JM049069Y